

Image Registered Gastroscopic Ultrasound (IRGUS) in human subjects: a pilot study to assess feasibility

Authors

K. L. Obstein¹, R. S. J. Estépar², J. Jayender³, V. D. Patil³, I. S. Spofford⁴, M. B. Ryan⁵, B. I. Lengyel², R. Shams⁶, K. G. Vosburgh^{2,3}, C. C. Thompson⁵

Institutions

Institutions are listed at the end of article.

submitted 20 July 2010
accepted after revision
10 December 2010

Bibliography

DOI <http://dx.doi.org/10.1055/s-0030-1256241>
Published ahead of print
Endoscopy
© Georg Thieme Verlag KG
Stuttgart · New York
ISSN 0013-726X

Corresponding author

C. C. Thompson, MD
Brigham and Women's Hospital
Division of Gastroenterology
75 Francis Street
Boston
MA 02115
USA
Fax: +1-617-264-6342
ccthompson@partners.org

Background and study aims: Endoscopic ultrasound (EUS) is a complex procedure due to the subtleties of ultrasound interpretation, the small field of observation, and the uncertainty of probe position and orientation. Animal studies demonstrated that Image Registered Gastroscopic Ultrasound (IRGUS) is feasible and may be superior to conventional EUS in efficiency and image interpretation. This study explores whether these attributes of IRGUS will be evident in human subjects, with the aim of assessing the feasibility, effectiveness, and efficiency of IRGUS in patients with suspected pancreatic lesions.

Patients and methods: This was a prospective feasibility study at a tertiary care academic medical center in human patients with pancreatic lesions on computed tomography (CT) scan. Patients who were scheduled to undergo conventional EUS were randomly chosen to undergo their procedure with IRGUS. Main outcome measures included feasibility, ease of use, system func-

tion, validated task load (TLX) assessment instrument, and IRGUS experience questionnaire.

Results: Five patients underwent IRGUS without complication. Localization of pancreatic lesions was accomplished efficiently and accurately (TLX temporal demand 3.7%; TLX effort 8.6%). Image synchronization and registration was accomplished in real time without procedure delay. The mean assessment score for endoscopist experience with IRGUS was positive (66.6 ± 29.4). Real-time display of CT images in the EUS plane and echoendoscope orientation were the most beneficial characteristics.

Conclusions: IRGUS appears feasible and safe in human subjects, and efficient and accurate at identification of probe position and image interpretation. IRGUS has the potential to broaden the adoption of EUS techniques and shorten EUS learning curves. Clinical studies comparing IRGUS with conventional EUS are ongoing.

Introduction

Image guidance technology has revolutionized diagnostic and therapeutic modalities by providing physicians with the means to navigate throughout the body guided by three-dimensional (3D) images [1,2]. Image guidance has been shown to improve traditional surgical disease management in the abdomen through more accurate intra-operative definition of therapeutic targets and by reducing the aggressiveness of treatment [3–15]. Image data can be constructed, registered, and displayed to provide easily used and intuitive support in endoscopic procedures. Image guidance technology has been utilized in endoscopy in a porcine model through the Image Registered Gastroscopic Ultrasound (IRGUS) system, which was found to be superior to conventional endoscopic ultrasound (EUS) in accuracy of endoscope position and in image interpretation [16]. Addi-

tionally, the IRGUS system demonstrated the potential to shorten the EUS learning curve and to broaden the adoption of the EUS technique by gastroenterologists [16]. The current study aimed to explore whether the attributes of the IRGUS system will be effective, efficient, and feasible in human patients with pancreatic lesions who are scheduled to undergo EUS.

Patients and methods

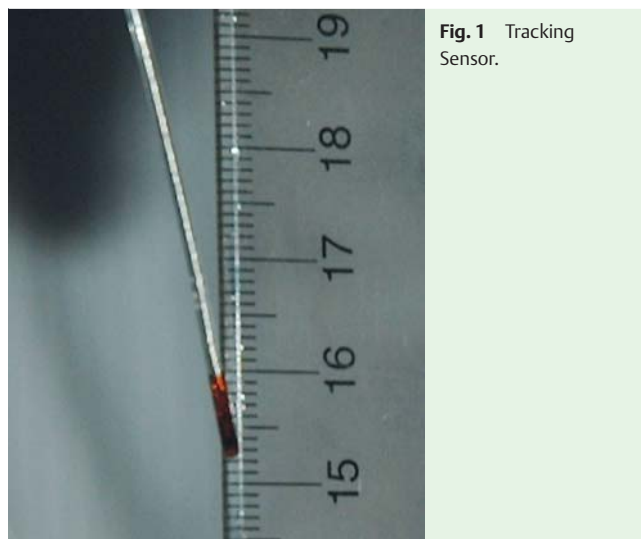
Patients with suspected pancreatic lesions on computed tomography (CT) scan and who were scheduled for EUS were identified for inclusion. From these patients, five who were scheduled to undergo conventional EUS were randomly chosen to undergo their procedure with the IRGUS system (► **Table 1**). The IRGUS system provides clinicians with a real-time display that shows endo-

Table 1 Patient characteristics.

Pa-tient	Age, years	Sex	Race	Indication for EUS
1	53	Female	Caucasian	57 × 43 mm mixed density lesion in the head of the pancreas
2	68	Male	Caucasian	39 × 32 mm ill-defined hypodense mass within the head of the pancreas
3	86	Male	Caucasian	31 × 14 mm predominately hypodense lesion in the tail of the pancreas extending anteriorly
4	40	Female	Caucasian	29 mm low attenuation lesion with thick rim and lack of obvious enhancement in the tail of the pancreas
5	54	Male	Caucasian	7 mm hypodense lesion projecting superiorly in the neck of the pancreas

scope position and ultrasound plane orientation within the pre-procedure volumetric CT images. For these five patients, two synthetic images (a 3D model of the reference anatomy and a single oblique planar slice that matches the plane sampled by the ultrasound transducer) were created from the CT images utilizing advanced customized visualization software (3D Slicer, www.slicer.org).

The IRGUS system uses established techniques for the visualization of the probe position and image registration, but implements them in real time by using recent advances in miniaturized position-tracking technology (microBIRD; Ascension Technology Corp, Milton, Vermont, USA). The tracking sensors are small (1 mm in diameter, 6 mm in length) and have been tested to meet International Electrotechnical Commission (IEC) 60601-01 standards (Fig. 1). The mini-sensors were sterilized within 24 h of the procedure according to the guidelines for surgical instruments and equipment at our center, by using the STERRAD sterilization system (Advanced Sterilization Products, Irvine, California, USA). All components (tracker system, interfaces, personal computer with displays) are commercially available, with a

**Fig. 1** Tracking Sensor.

total cost, depending on the size of the display, of under US \$19000.

Prior to the procedure, a standard patient stretcher was outfitted with an electromagnetic flat-plate transmitter (Fig. 2). The patient was then placed over the embedded transmitter and, immediately prior to patient sedation in the endoscopy suite, one miniature sensor was attached to the distal tip of a standard linear echoendoscope (GF-UC-140P-AL5, Olympus, Tokyo, Japan) using a combination of Steri-Strips and Tegaderms (3M, St. Paul, Minnesota, USA). The echoendoscope with attached sensor was then inserted into an Aloka SSD-α10 ultrasound console (Aloka Inc., Tokyo, Japan) (Fig. 3) and calibrated using an additional nonattached sensor. The calibration defines the coordinates of the ultrasound plane with respect to the coordinate frame of the attached sensor. Calibration was performed by touching the distal point of the echoendoscope to the nonattached sensor. The 3D body model of the patient was then registered to the CT coordinate system by scanning the patient's torso with the nonattached sensor to obtain a series of points. Those points were aligned to a 3D model of the patient's skin extracted from the CT using the iterative closest point algorithm [17].

**Fig. 2** Standard patient stretcher outfitted with the electromagnetic flat-plate transmitter. **a** The transmitter (white arrow) is positioned on the stretcher. **b** Padding is then used to cover the transmitter, making it comfortable for patients to lie upon.

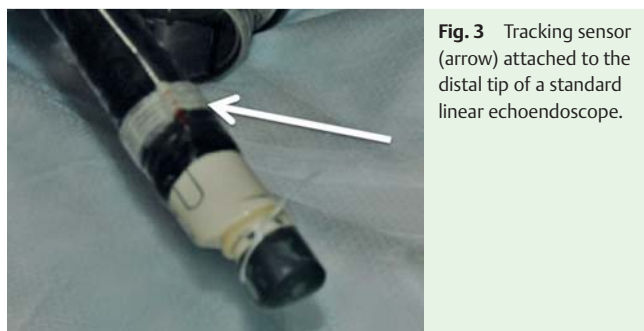


Fig. 3 Tracking sensor (arrow) attached to the distal tip of a standard linear echoendoscope.

The echoendoscope with the IRGUS system was then utilized for the endoscopic examination of the five patients by a single attending physician skilled in EUS and advanced endoscopic techniques.

Following each procedure, a validated task load (TLX) assessment instrument (NASA Task Load Index v1.0, NASA Ames Research Center, Moffett Field, California, USA) and an IRGUS experience questionnaire were completed. The TLX is a subjective workload assessment technique commonly used in human factors research to assess perceived workload based on a multidimensional construct of six subscales: mental demand (how much mental and perceptual activity was required?), physical demand (how much physical activity was required?), temporal demand (how hurried or rushed was the pace of the task?), performance (how successful were you in accomplishing what you were asked to do?), effort (how hard did you have to work to accomplish your level of performance?), and frustration level (how insecure, discouraged, irritated, stressed, and annoyed were you?) [18–20]. The TLX has been used to assess workload in transportation (ground and aviation), endurance tasks, healthcare, teaching, and power plants [20–27]. The TLX can be weighted or unweighted, and each subscale ranges from 0 to 100. We chose to use the unweighted TLX subscale scores in this research study, as they have been more commonly used and there is high correlation between the weighted and unweighted scores [28,29]. All cases were recorded in .avi format, de-identified, and stored on a secure, encrypted, workstation at the medical center for review and analysis.

This research study was approved by the center's Institutional Review Board (IRB) and was funded through a grant from the National Cancer Institute under award R42 CA115112-03, the National Center for Image Guided Therapy under award U41 RR019703, and the Center for Integration of Medicine and Innovative Technology (CIMIT).

Results

The five human patients underwent their procedure with use of the IRGUS system safely and without complication. All procedures were performed in the endoscopy suite with intravenous sedation (propofol administered by an anesthesiologist [n = 2] or midazolam and fentanyl administered by the endoscopy team [n = 3]). Endoscopic examination (including Doppler evaluation) was carried out with complete exploration of the pancreas (head, body, and tail). Localization of the pancreatic lesion was accomplished efficiently and accurately (Table 2).

Image synchronization and registration was accomplished by a short calibration process at the beginning of the procedure, prior to the insertion of the echoendoscope. Synchronization was ac-

Table 2 Unweighted Task Load Index subscale rating for Image Registered Gastroscopy Ultrasound (IRGUS). All subscales range from 0 (“very low”) to 100 (“very high”); the exception is the subscale of “Performance”, where 0 is “perfect” and 100 is “failure”.

Subscale	Unweighted rating, median (range)
Mental Demand	65 (25–90)
Physical Demand	45 (20–75)
Temporal Demand	55 (25–75)
Performance	30 (10–80)
Effort	35 (20–80)
Frustration	20 (15–80)

complished in 3–4 s, and registration was accomplished in 2–4 min. Retroperitoneal structures remained localized in position relative to stable structures such as the aorta. The precise registration of the 3D image and endoscope position was minimally distorted for structures in the right upper quadrant when the patient was in the left-lateral decubitus position. The distortion or targeting error, defined as the distance between the line defined by the needle and the lesion center, was 12.23 ± 0.45 mm for a lesion diameter of 21.38 mm. The accuracy of registration in the pancreas was affected by endoscope location, with improved registration in the stomach compared with registration in the duodenum.

The mean assessment score for endoscopist experience with IRGUS was positive (66.6 ± 29.4), and IRGUS was favored as providing an advantage over conventional EUS (65 ± 26.5). Real-time display of CT images in the EUS plane and echoendoscope orientation were the most beneficial characteristics of IRGUS (Figs. 4, 5).

Discussion

In the current study, IRGUS appears feasible and safe in human subjects. All patients tolerated the examination well without procedural delay. The system did not encumber the endoscopist or the endoscopy suite staff. The system uses pre-existing equipment in the endoscopy suite (patient stretchers, echoendoscopes, mouth-guards) and was simple to assemble immediately prior to the procedure without difficulty. In short, the IRGUS system has the potential to be practical in the “real-life” high-volume endoscopy suite setting.

The IRGUS system was efficient and accurate at identification of probe position and image interpretation. This allowed the endoscopist to quickly visualize anatomic structures without losing echoendoscope image orientation (especially when the echoendosonographic image is degraded by calcifications, artifacts, or poor surface contact). This may promote shortened procedure times, therefore decreasing sedation requirements, and improving patient safety. Use of the IRGUS system may also lead to improvement in lesion targeting for echoendoscopic biopsy or fine-needle aspiration, with the potential to enhance tissue sampling for better diagnosis of disease.

While retroperitoneal structures remained localized in position, the precise registration of the 3D image and endoscope position were minimally distorted (12.23 ± 0.45 mm for a lesion diameter of 21.38 mm) for structures in the right upper quadrant when the patient was in the left-lateral decubitus position. This distortion or target error is within the bounds that can make the guidance

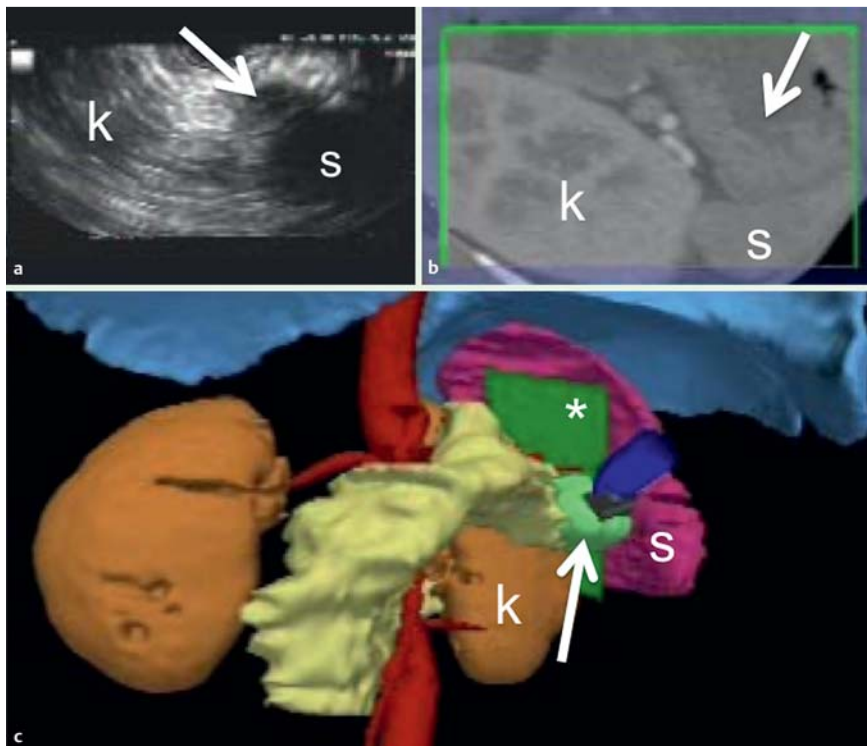


Fig. 4 The actual Image Registered Gastroscope Ultrasound (IRGUS) system real-time display with: **a** ultrasound image; **b** reformatted computed tomography (CT) image in the ultrasound-defined plane; **c** 3D CT-based model of the patient, all on the same monitor for navigation and orientation. The ultrasound image plane (*) cuts directly through the pancreatic lesion (arrows). k, left kidney; s, spleen.

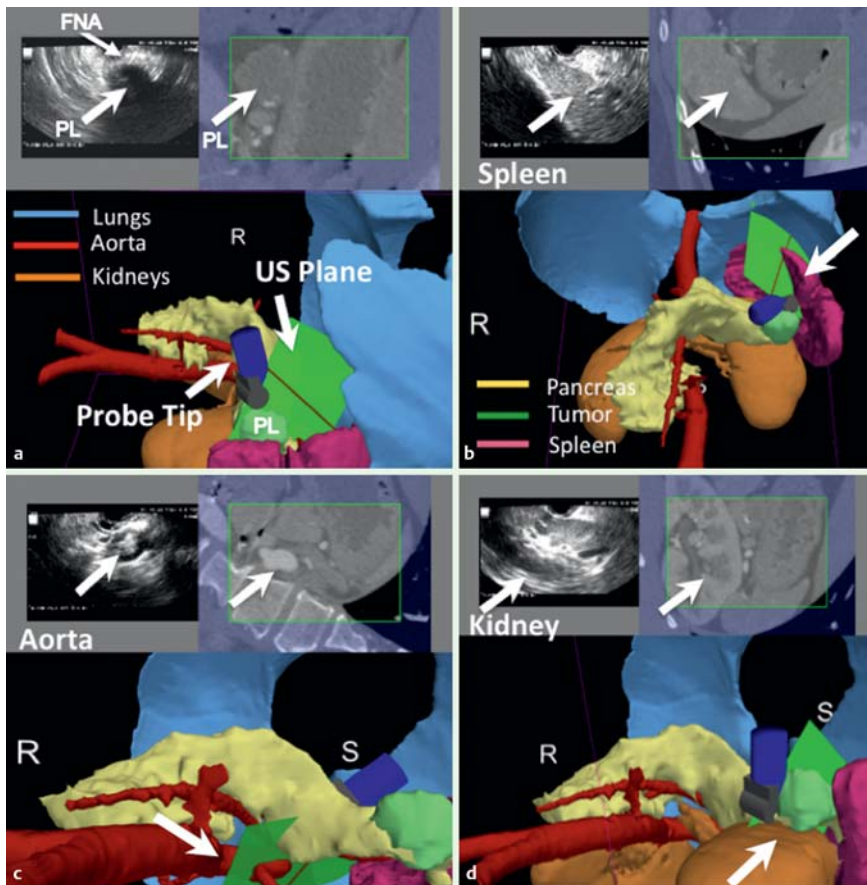


Fig. 5 The actual Image Registered Gastroscope Ultrasound (IRGUS) system real-time display (different patient than Fig. 4). **a** The endoscopic ultrasound probe tip, ultrasound plane (US plane), pancreatic lesion (PL), fine-needle aspiration needle (FNA), lungs (blue), aorta (red), and kidneys (brown) are clearly visualized. **b** The spleen (white arrows) can be seen on the computed tomography image, 3D model, and ultrasound image in the same plane as the ultrasound. **c** The aorta is demonstrated in the image plane (white arrows). **d** The left kidney is clearly visualized in the image plane (white arrows). R, right; S, superior.

system clinically useful. A detailed validation study of targeting accuracy is currently underway. The precision of registration was also affected by endoscope endoluminal location, with improved registration in the stomach compared with registration in the duodenum.

The 3D reconstruction (segmentation) process for the procedure is semi-automatic (a supervised combination of imaging techniques) and may be accomplished by an individual with basic computer literacy. Based on the system used for this research study, the time for segmentation ranges from 30 min to 1.5 h, depending on the file size of the images. This time may be streamlined to approximately 15 min by increasing computer processor speed and system memory. The 3D reconstruction simplifies image interpretation (both CT images and ultrasound images) for the endoscopist and may promote shortened procedure times. Due to the intuitive nature in visualizing the 3D anatomy, no learning curve was demonstrated and no additional training in 3D anatomy is necessary to use the image guidance system.

A potential technical limitation was the registration error of the synthesized oblique CT image to the ultrasound image planes of approximately 5 mm. IRGUS capability does not depend on absolute image registration accuracy, therefore this minimal shift was found to be sufficient, as most targets for orientation are considerably larger and slight misregistrations did not appear to hamper the use of the system. Because the 3D and CT images of the system are based on a pre-procedure CT scan, they are static. Therefore, when a pancreatic cyst is drained, it resolves on the ultrasound image but remains on the 3D reconstruction and CT images. While it would provide further information to have dynamic radiologic images, it would also expose the patient to additional unnecessary radiation and be more difficult for widespread system adoption. Not having the dynamic images may also prove to be an advantage, as the endosonographer is able to visualize the site of intervention as it looked before intervention. This may assist the endoscopist in maintaining orientation and allowing for a careful examination of the area that was known to have the finding of interest.

We also anticipated that the motion of organs induced by respiration and gravity would compromise the utility of the comparison of the preoperative CT image with the real-time ultrasound image. This was not the case, as very little relative motion (~3 mm) between the CT oblique image and the US image was observed. When the patient was in the left-lateral decubitus position, gravity did cause minimal distortion between the CT image and the real-time ultrasound image for structures that were in the left upper quadrant. However, all retroperitoneal structures and structures in the right side remained in position without distortion. Finally, the current study was a feasibility study of five human patients and a single endoscopist. Larger, randomized, clinical studies comparing IRGUS with conventional EUS with multiple operators are ongoing.

In summary, IRGUS appears feasible and may be superior to conventional EUS in accuracy of probe positioning and in image interpretation; however, these comparisons are limited in the current feasibility study. When considering these results, as well as the intuitive interface and the ease of implementation, it is anticipated that such systems could find utility in many diagnostic and therapeutic endoscopic procedures, including the potential for the development of new procedures with novel indications. These preliminary results also suggest that IRGUS technology may shorten the EUS learning curve and could broaden the adoption of EUS techniques.

Competing interests: None

Institutions

- ¹ Division of Gastroenterology, Vanderbilt University Medical Center, Nashville, Tennessee, USA
- ² Surgical Planning Laboratory, Brigham and Women's Hospital, Boston, Massachusetts, USA
- ³ Center for Integration of Medicine and Innovative Technology Image Guidance Laboratory, Massachusetts General Hospital, Boston, Massachusetts, USA
- ⁴ Division of Pediatric Gastroenterology, Massachusetts General Hospital, Boston, Massachusetts, USA
- ⁵ Division of Gastroenterology, Brigham and Women's Hospital, Boston, Massachusetts, USA
- ⁶ College of Engineering and Computer Science, Australian National University, Canberra, Australian Capital Territory, Australia

References

- ¹ Peters T, Cleary K, eds. Image-guided interventions: technology and applications. 1st edn. New York: Springer Science+Business Media; 2008: 1–560
- ² Vosburgh KG, Jolesz FA. The concept of image-guided therapy. *Acad Radiol* 2003; 10: 176–179
- ³ Brugge WR. Fine needle aspiration of pancreatic masses: the clinical impact. *Am J Gastroenterol* 2002; 97: 2701–2702
- ⁴ Kane R. Intraoperative ultrasonography: history, current state of the art, and future directions. *J Ultrasound Med* 2004; 23: 1407–1420
- ⁵ Rösch T, Lorenz R, Braig C et al. Endoscopic ultrasound in pancreatic tumor diagnosis. *Gastrointest Endosc* 1991; 37: 347–352
- ⁶ Di Stasi M, Lencioni R, Solmi L. Ultrasound-guided fine needle biopsy of pancreatic masses: results of a multicenter study. *Am J Gastroenterol* 1998; 93: 1329–1333
- ⁷ Rattner DW, Fernandez-del Castillo C, Brugge WR et al. Defining the criteria for local resection of ampullary neoplasms. *Arch Surg* 1996; 131: 366–371
- ⁸ Ellsmere J, Stoll J, Wells 3rd W et al. A new visualization technique for laparoscopic ultrasonography. *Surgery* 2004; 136: 84–92
- ⁹ Ambardar S, Arnell TD, Whelan RL et al. A preliminary, prospective study of the usefulness of a magnetic endoscope locating device during colonoscopy. *Surg Endosc* 2005; 19: 897–901
- ¹⁰ Shah SG, Brooker JC, Thapar C et al. Effect of magnetic endoscope imaging on patient tolerance and sedation requirements during colonoscopy: a randomized controlled trial. *Gastrointest Endosc* 2002; 55: 832–837
- ¹¹ Shah SG, Saunders BP, Brooker JC et al. Magnetic imaging of colonoscopy: an audit of looping, accuracy and ancillary maneuvers. *Gastrointest Endosc* 2000; 52: 1–8
- ¹² Schwarz Y, Mehta AC, Ernst A et al. Electromagnetic navigation during flexible bronchoscopy. *Respiration* 2003; 70: 516–522
- ¹³ Herth FJ, Ernst A, Eberhardt R et al. Endobronchial ultrasound-guided transbronchial needle aspiration of lymph nodes in the radiologically normal mediastinum. *Eur Respir J* 2006; 28: 910–914
- ¹⁴ Shen SH, Fennessy F, McDannold N et al. Image-guided thermal therapy of uterine fibroids. *Semin Ultrasound CT MR* 2009; 30: 91–104
- ¹⁵ Dimaio SP, Archip N, Hata N et al. Image-guided neurosurgery at Brigham and Women's Hospital. *IEEE Eng Med Biol Mag* 2006; 25: 67–73
- ¹⁶ Vosburgh KG, Stylopoulos N, San Jose Estepar R et al. EUS with CT improves efficiency and structure identification over conventional EUS. *Gastrointest Endosc* 2007; 65: 866–870
- ¹⁷ Besl P, McKay N. A method for Registration of 3-D Shapes. *IEEE Transactions on Pattern Analysis and Machine Intelligence (PAMI)* 1992; 14: 239–256
- ¹⁸ Cao A, Chintamani KK, Pandya AK, Ellis RD. NASA TLX: software for assessing subject mental workload. *Behavior Research Methods* 2009; 41: 113–117
- ¹⁹ Hart SG, Staveland LE. Development of NASA-TLX (Task Load Index): results of empirical and theoretical research. In: Hancock PA, Meshkati N, eds. Human mental workload. Amsterdam: Elsevier; 1988: 139–183
- ²⁰ Saleem JJ, Patterson ES, Militello L et al. Impact of clinical reminder redesign on learnability, efficiency, usability, and workload for ambulatory clinic nurses. *J Am Med Inform Assoc* 2007; 14: 632–640

- 21 Temple JG, Warm JS, Dember WN *et al.* The effects of signal salience and caffeine on performance, workload, and stress in an abbreviated vigilance task. *Hum Factors* 2000; 42: 183–194
- 22 Hakan A, Nilsson L. The effects of a mobile telephone task on driver behavior in a car following situation. *Acc Anal Prev* 1995; 27: 707–715
- 23 Averty P, Collet C, Dittmar A *et al.* Mental workload in air traffic control: an index constructed from field tests. *Aviat Space Environ Med* 2004; 75: 333–341
- 24 Park J, Jung W. A study on the validity of task complexity measure of emergency operating procedures of nuclear power plants – comparing with a subjective workload. *IEEE Trans Nucl Sci* 2006; 53: 2962–2970
- 25 Oginska H, Fafrowicz M, Golonka K *et al.* Chronotype, sleep loss, and diurnal pattern of salivary cortisol in a simulated daylong driving. *Chronobiology International* 2010; 27: 959–974
- 26 Carswell CM, Lio CH, Grant R *et al.* Hands-free administration of subjective workload scales: acceptability in a surgical training environment. *Appl Ergon* 2010; 42: 138–145
- 27 Levin S, France DJ, Hemphill R *et al.* Tracking workload in the emergency department. *Hum Factors* 2006; 48: 526–539
- 28 Byers JC, Bittner AC, Hill SG. Traditional and raw task load index (TLX) correlations: are paired comparisons necessary? In: Mital A, ed. *Advances in industrial ergonomics and safety I*. London: Taylor & Francis; 1989: 481–485
- 29 Moroney WF, Biers DW, Eggemeier FT, Mitchell JA. A comparison of two scoring procedures with the NASA Task Load Index in a simulated flight task. *Proceedings of the IEEE* 1992; 2: 734–740